Chemistry & Biology
Article

Alkyl-CoA Disulfides as Inhibitors and Mechanistic Probes for FabH Enzymes

Mamoun M. Alhamadsheh,[1] Faik Musayev,[2,3] Andrey A. Komissarov,[1] Sarbjot Sachdeva,[1,2,3] H. Tonie Wright,[2,4] Neel Scarsdale,[2,4] Galina Florova,[1] and Kevin A. Reynolds[1,*]
[1] Department of Chemistry, Portland State University, Portland, OR 97207, USA
[2] Institute of Structural Biology and Drug Discovery
[3] Department of Medicinal Chemistry
[4] Department of Biochemistry
Virginia Commonwealth University, Richmond, VA 23219, USA
*Correspondence: reynoldsk@pdx.edu
DOI 10.1016/j.chembiol.2007.03.013

SUMMARY

The first step of the reaction catalyzed by the homodimeric FabH from a dissociated fatty acid synthase is acyl transfer from acyl-CoA to an active site cysteine. We report that C_1 to C_{10} alkyl-CoA disulfides irreversibly inhibit *Escherichia coli* FabH (ecFabH) and *Mycobacterium tuberculosis* FabH with relative efficiencies that reflect these enzymes' differential acyl-group specificity. Crystallographic and kinetic studies with MeSSCoA show rapid inhibition of one monomer of ecFabH through formation of a methyl disulfide conjugate with this cysteine. Reaction of the second subunit with either MeSSCoA or acetyl-CoA is much slower. In the presence of malonyl-ACP, the acylation rate of the second subunit is restored to that of the native ecFabH. These observations suggest a catalytic model in which a structurally disordered apo-ecFabH dimer orders on binding either the first substrate, acetyl-CoA, or the inhibitor MeSSCoA, and is restored to a disordered state on binding of malonyl-ACP.

INTRODUCTION

Fatty acid biosynthesis, an essential and universal process for cell membrane generation and maintenance, is carried out by two related but distinct de novo fatty acid synthase (FAS) systems. Eukaryotes utilize a large multifunctional protein with one or two polypeptides (type I FAS system) [1–3], whereas the type II FAS system of plants, prokaryotes, and protozoa is composed of discrete monofunctional enzymes with activities that correspond to the domains of the type I single-chain FAS [4–6]. These significant differences in structure and organization of the type I and II FAS systems have distinguished the type II FAS enzymes as potential targets for development of novel antibacterial and antiparasitic agents that might have minimal side effects in humans [7–9].

β-ketoacyl-ACP-synthase III (FabH) is a key enzyme in bacterial fatty acid biosynthesis [4, 10], catalyzing the committed step of the synthesis cycle. It initiates fatty acid biosynthesis via a cysteine-mediated Claisen condensation reaction between malonyl-acyl carrier protein (MACP) and an acyl-enzyme intermediate formed by initial transacylation from the acyl-CoA primer to the active site Cys112 [10]. CoA is released from the enzyme after transacylation and replaced by MACP in the same binding pocket. FabH then catalyzes the decarboxylation of MACP, which reacts with the Cys112-bound acyl group to form β-ketoacyl-ACP. This product is released, reduced to the corresponding acyl-ACP, and subsequently elongated by other FAS condensing enzymes, including FabB and FabF [11].

Of the known inhibitors of type II FAS enzymes, most target enzymes other than FabH [12]. Cerulenin, thiolactomycin, and phomallenic acids inhibit FabB and FabF. Cerulenin forms a covalent adduct with the active site cysteine of FabF [13, 14], while thiolactomycin acts as a reversible inhibitor [8, 15, 16]. Recently, a number of new inhibitor classes including indole-based inhibitors [17], 1,2-dithiole-3-ones [18], substituted thiazolidine-2-ones [19], and benzoylaminobenzoic acid derivatives [20] that target FabH have been discovered. These discoveries have exploited the crystal structures of FabH from several bacterial species [17, 21–29] and FabH assays amenable to high-throughput screens [30].

The buried active site of FabH, consisting of the Cys112, His244, and Asn274 catalytic triad, lies at the base of a narrow channel in which CoA binds. Crystal structures have revealed that both the indole-based and benzoylaminobenzoic acid FabH inhibitors bind in this channel [17, 20]. In the latter case, there also appears to be an interaction of an inhibitor carboxylate with an active site Asn. None of the inhibitors reported to date interacts with the active site Cys112. This residue forms the acyl enzyme intermediate from the corresponding acyl-CoA substrate, with release of CoA, and mutational analysis has shown that this residue is critical for the condensing activity of FabH [28, 29, 31, 32]. Selective chemical modification of

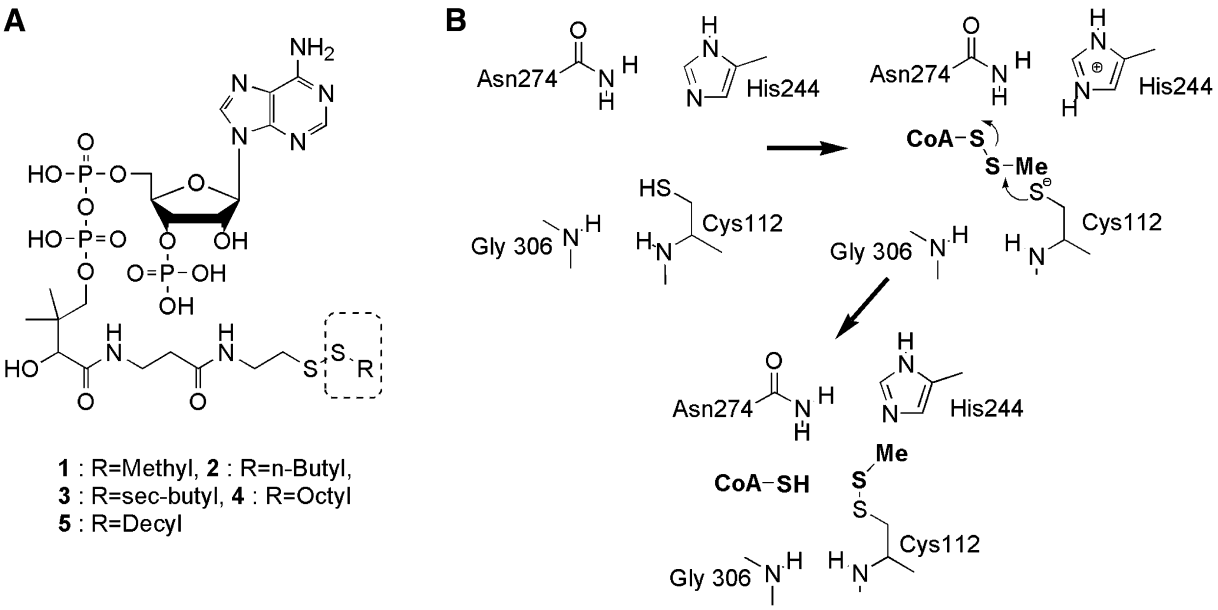

Figure 1. FabH Inhibition by Alkyl-CoA Disulfides

(A) Chemical structures of alkyl-CoA disulfides **1**–**5**.

(B) Proposed mechanism of ecFabH inactivation by MeSSCoA (**1**). Cys112 of ecFabH forms a methyl disulfide conjugate upon incubation with MeSS-CoA (**1**). The released CoA in the CoA binding channel may be retained or dissociated.

Cys112 through formation of a mixed disulfide would thus be expected to render the enzyme inactive.

FabHs from different bacterial species show different substrate specificities for the acyl-CoA primer: the *Escherichia coli* and *Mycobacterium tuberculosis* enzymes (ecFabH and mtFabH) are specific for acetyl-CoA and lauroyl-CoA, respectively [27, 33–37]. This specificity is conferred by the size and shape of the acyl binding pockets of these enzymes, which have been determined from crystal structures. Because Cys112 sits at the juncture of the CoA and acyl binding channels, inhibitors that target this residue and contain structural components for both the CoA and acyl binding channel might allow for predictable selective inhibition of FabH enzymes.

Alkyl-CoA disulfides have been used previously as inhibitors and probes of choline acetyltransferase [38–43] and spermidine/spermine acetyltransferases [44]. Currier and Mautner demonstrated that methyl-CoA disulfide is a potent competitive inhibitor of choline acetyltransferase, and they proposed that the methyl-CoA disulfide (MeSS-CoA) forms a tight complex with the enzyme without undergoing chemical reaction [38, 39]. We hypothesized that alkyl-CoA disulfides should act as FabH inhibitors through formation of a mixed disulfide with the active site Cys112, if the pKa of the cysteine-SH group is low enough. The CoA group should provide a specificity determinant directing the disulfide to the active site residue, while the alkyl group would confer specificity for a FabH enzyme.

As a test of our hypothesis, we have synthesized C_1–C_{10} alkyl-CoA disulfides (Figure 1A) and shown that they give predictable differential inhibition of ecFabH and mtFabH. Crystal structures show formation of a covalent methyl disulfide bond at one active site cysteine in the ecFabH dimer. These crystal structures in conjunction with a series of kinetic binding and inhibition studies are consistent with a catalytic model for FabH that involves structural changes which accompany both substrate binding and product release.

RESULTS AND DISCUSSION

Synthesis of Alkyl-CoA Disulfides 1–5

MeSSCoA (**1**) has previously been generated by reacting the trilithium salt of CoA with an excess of S-methylmethanethiosulfonate in water, with subsequent purification using a Sephadex G-10 column [38, 39]. This procedure proved problematic for synthesis of longer (C_8 or C_{10}) alkyl-CoA disulfides due to solubility and purification difficulties and was modified (see Figure S1 in the Supplemental Data available with this article online) to use the trihydrate of CoA and perform the coupling reaction (with the corresponding S-alkylmethanethiosulfonate reagent) in anhydrous methanol. When the reaction reached completion (monitored by either reverse-phase HPLC or TLC), the excess of the reagent was removed by solvent extraction. The alkyl-CoA disulfides (**1**–**5**; Figure 1) were then purified on a C18 cartridge, and their identity was confirmed by ^{1}H NMR and high-resolution mass spectrometry (HRMS) analysis (see Supplemental Data). This modified procedure was robust and is likely applicable for the synthesis of a wide range of alkyl-CoA disulfides.

Table 1. IC_{50} for Alkyl-CoA Disulfides 1–5 against ecFabH and mtFabH

Alkyl-CoA Disulfide	ecFabH IC_{50} (μM)[a]	mtFabH IC_{50} (μM)[b]
Methyl-CoA disulfide **1**	57.1 ± 4.5	>300
Butyl-CoA disulfide **2**	>300	>300
Sec-butyl-CoA disulfide **3**	>300	>300
Octyl-CoA disulfide **4**	>300	30.1 ± 5.2
Decyl-CoA disulfide **5**	>300	1.2 ± 0.7

IC_{50}, concentration of inhibitor at which 50% inhibition of FabH activity is achieved.
[a] Inhibitors were preincubated with ecFabH for 15 min at room temperature before assay.
[b] IC_{50} was determined without preincubation.

Differential Inhibition of ecFabH and mtFabH by Alkyl-CoA Disulfides 1–5

The effects of alkyl-CoA disulfides on the activity of ecFabH and mtFabH were initially studied by incubating the inhibitors with FabH for 15 min at room temperature and then using standard assay conditions described previously [10, 29, 33, 45]. While MeSSCoA (**1**) inhibited ecFabH (IC_{50} = 57.1 ± 4.5 μM), the disulfides with the largest alkyl groups (**4** and **5**) showed no significant inhibitory activity at concentrations as high as 300 μM (Table 1). Conversely, the longest-chain alkyl-CoA disulfides, octyl-CoA (**4**) (IC_{50} 30.1 ± 5.2 μM) and decyl-CoA (**5**) (IC_{50} 1.2 ± 0.7 μM), were active against mtFabH, while **1** exhibited no inhibition of mtFabH at 300 μM (Table 1). At these concentrations, there was no inhibition of mtFabH or ecFabH by either butyl-CoA disulfide (**2**) with an intermediate-size alkyl group or by the branched-chain sec-butyl-CoA disulfide (**3**).

These specificities for the acyl-CoA disulfide inhibitors parallel those for the acyl-CoA substrates of these enzymes [24, 29, 35, 36, 46]. mtFabH reacts only with long-chain (C_{10}–C_{16}) acyl-CoAs and has a long internal acyl binding channel extending from the active site cysteine [28]. In ecFabH, this channel is obstructed by Phe87 from the other subunit (which is a threonine in mtFabH), leaving a pocket that can accept only acetyl- or propionyl-CoA substrates [24, 35, 36]. The initial hypothesis that differential inhibition of FabH by alkyl-CoA disulfides of varying alkyl chain length correlates with their acyl-CoA substrate preferences is borne out and is consistent with the alkyl group of the inhibitor binding in the FabH acyl channel.

Cysteine Modification in ecFabH by MeSSCoA (1)

The alkyl-CoA disulfides were designed to target the catalytically important Cys112 of FabH via a sulfhydryl-disulfide exchange. We observed that ecFabH was inhibited only by MeSSCoA (**1**) and that the presence of acetyl-CoA provided protection against inhibition, consistent with modification of the active site cysteine. An investigation of the reversibility of this inhibition provided evidence that this modification was formation of a disulfide bond. ecFabH with MeSSCoA (**1**) were incubated under conditions that resulted in greater than 85% loss of enzyme activity. No significant activity was recovered when the inhibited protein was dialyzed (12 hr in 50 mM phosphate buffer at pH 7.4 and 4°C) or purified by gel filtration. In contrast, enzyme treated by reversible inhibitors regained full activity under these conditions. Treatment of the inhibited protein with 10 mM dithiothreitol for 30 min prior to dialysis resulted in complete restoration of enzyme activity, confirming the presence of an active site cysteine disulfide linkage. X-ray crystallographic studies (described below) confirmed formation of this disulfide linkage and demonstrate that it involves the methyl thiol (Figure 1B) and not the CoA thiol.

Fluorimetric Studies of a Fast Reaction between ecFabH and MeSSCoA (1)

Stopped-flow fluorimetry was employed to monitor the initial fast stages of interaction between ecFabH and MeSSCoA (**1**). As described below for the ecFabH-MeSSCoA crystal structure and as also observed in the structure of ecFabH-CoA complexes, the adenine ring of the CoA is stacked between the indole side chain of Trp32 and the guanidine group of Arg151, suggesting that changes in Trp fluorescence emission might report interactions at the ecFabH binding site. Indeed, fast mixing of the ecFabH (0.5 μM) with MeSSCoA (**1**) (150 μM) revealed an initial fast decrease ($t_{1/2}$ ~0.06 s) in Trp fluorescence emission followed by a relatively slow ($t_{1/2}$ ~5 s) increase (Figure 2A). These changes are likely associated with binding and inhibition of ecFabH, as BuSSCoA (**2**) does not inhibit ecFabH (Table 1) and shows no effect on Trp fluorescence (Figure 2A). Acetyl-CoA also did not cause a change in Trp fluorescence (Figure 2A), indicating that there are differences in the initial binding steps of inhibitor **1** and substrate.

The changes in tryptophan fluorescence emission at early times in the reaction were measured over a range of MeSSCoA (**1**) concentrations (0–150 μM). The observed rate constants (k_{obs}) for both the decrease and increase in fluorescence emission were determined by fitting a single exponential equation to each corresponding trace as described in Experimental Procedures. These rate constants were then plotted versus concentration of MeSSCoA (Figure 2B). The MeSSCoA (**1**) concentration dependence of k_{obs} for the fast decrease in Trp fluorescence demonstrated saturation at concentrations higher than 100 μM (Figure 2B), indicating a fast reversible binding (formation of E~I in Figure 3A) followed by a unimolecular transition (formation of E-I in Figure 3A). Fitting a hyperbolic equation to the data obtained for the fast step of the reaction gave the kinetic constants k_{lim} = 11.8 ± 1.4 s^{-1} and $K_{0.5}$ = 120 ± 30 μM. In contrast, the step detected by an increase in Trp fluorescence emission was slower (k_{slow} = 0.14 s^{-1}) and did not change significantly through the whole range of concentrations of MeSSCoA (**1**) studied (Figure 2B). This slow unimolecular step is tentatively assigned to the E-I to E-I* conversion in Figure 3A.

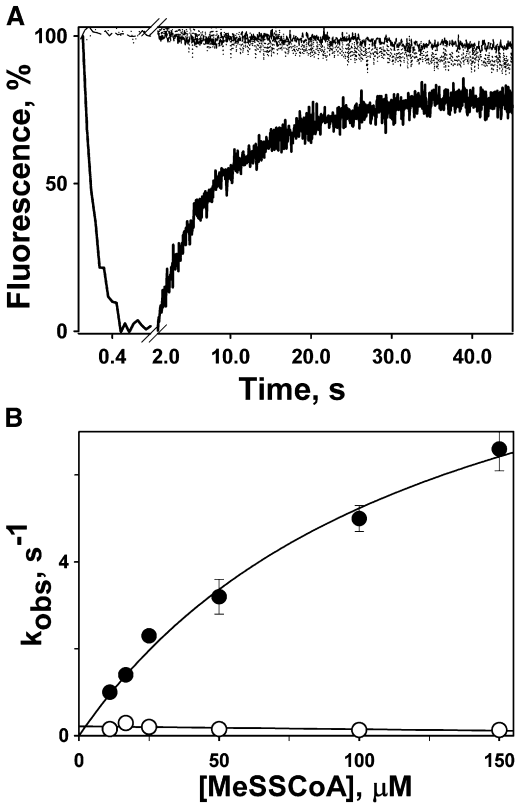

Figure 2. Fluorescence Kinetics for Interaction of ecFabH with MeSSCoA, BuSSCoA, and Acetyl-CoA

(A) Time dependencies of changes in ecFabH (0.5 μM) Trp fluorescence (excitation 290 nm) emission is observed only with 150 μM MeSSCoA (**1**) (darkest trace) and not with 150 μM acetyl-CoA or BuSSCoA (**2**) (other traces).

(B) The dependence of k_{obs} for the fast (●) and slow (○) steps of the reaction of ecFabH with MeSSCoA (**1**) on the concentration of the inhibitor. Values of k_{obs} for the fast (0–2 s) and slow (2–50 s) steps of the reaction of ecFabH with MeSSCoA (**1**) were calculated by fitting a single exponential equation to time traces of changes in the Trp fluorescence emission observed for each step, as described in Experimental Procedures.

These fluorescence studies suggest that the initial steps of interaction of MeSSCoA (**1**) with ecFabH involve a reversible binding dependent on inhibitor concentration, followed by a fast and then a slow step. The rates for these changes indicate that under saturating concentrations of MeSSCoA, formation of E-I* will be complete in less than 1 min. As described below, this E-I* retains 50% enzymatic activity.

ecFabH Undergoes Biphasic Inhibition with MeSSCoA (1) and Biphasic Acylation with Acetyl-CoA

Initial experiments showing that MeSSCoA (**1**) was the only ecFabH inhibitor in the panel of alkyl-CoA disulfides were carried out using a 15 min preincubation with ecFabH. In the absence of this preincubation, MeSSCoA was less effective (IC_{50} 111.3 ± 4.2 μM), suggesting a slow time-dependent inhibition step. A time course of inactivation of ecFabH at varying concentrations of MeSSCoA (**1**) (1–50 μM) (Figure 4A) provided support for this hypothesis. At inhibitor concentrations above 10 μM, there was an initial fast partial inactivation of the enzyme followed by a slower loss of activity (Figure 4A).

The fast step ($k_{i1} > 0.023\ s^{-1}$; Figure 3B) appears to be dependent on MeSSCoA (**1**) concentration (Figure 4A) and reaches a maximum of 50% inactivation (even with 400 μM MeSSCoA). The kinetic steps leading to E-I* (Figure 3A) revealed by fluorimetry reflect in part or whole the steps which lead to this 50% inactivated complex (E-I′; Figure 3B). Prolonged saturating conditions led to slow, complete (more than 99%) loss of all enzymatic activity (formation of $E\text{-}I_2$ in Figure 3B). Kinetic constants for the slow inhibition step, estimated by fitting a hyperbolic equation to the data shown in Figure 4A, are $k_{i2} = 2.5 \pm 0.3 \times 10^{-4}\ s^{-1}$ and $K_i = 37 \pm 11$ μM. This biphasic inhibition and 50% maximal inactivation in the fast step is consistent with fast modification of the active site cysteine of one subunit of the ecFabH dimer, followed by a much slower modification of the corresponding residue in the second subunit. As described below, crystal structures show the MeS group substituted on only one of the two subunits in the ecFabH dimer. The different modification rates (there is more than a 90-fold difference between k_{i1} and k_{i2}) might reflect changes resulting from modification of one subunit or intrinsic differences between the two subunits.

A similar biphasic process was seen for diacylation of the ecFabH dimer by the acetyl-CoA substrate (Figure 4B). We measured the rate of acylation of ecFabH with saturating concentrations of [^{14}C]acetyl-CoA over a 10 min period (Figure 4B). There was a fast monoacylation of ecFabH within 10 s of starting the reaction. Within 2 min, the FabH dimer was almost completely radiolabeled by two acetyl-CoA molecules (100% acylation). The assay

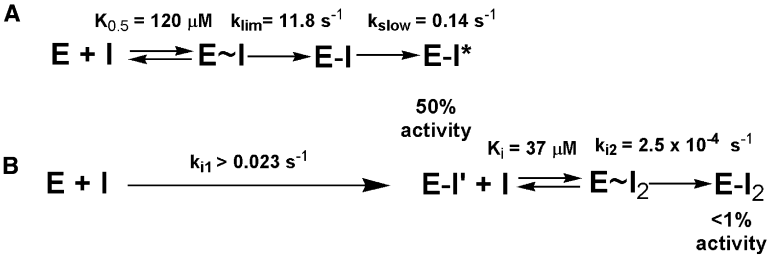

Figure 3. Kinetic Analysis of Inhibition of ecFabH by MeSSCoA

E, ecFabH; I, MeSSCoA.

(A) Steps observed by changes in Trp fluorescence emission of ecFabH.

(B) Steps observed by loss of ecFabH activity. See text for details.

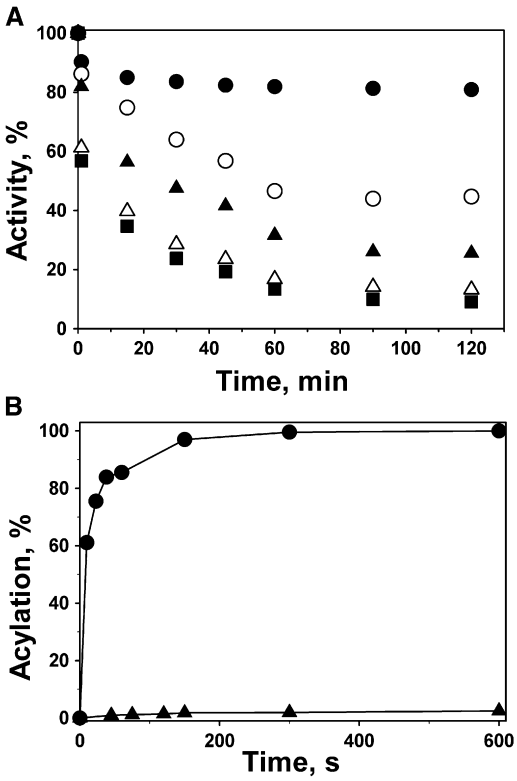

Figure 4. Biphasic Inhibition of ecFabH by MeSSCoA (1) and Biphasic Acylation by [^{14}C]Acetyl-CoA

(A) ecFabH (0.5 μM) was incubated with 1 (●), 3 (○), 5 (▲), 10 (Δ), and 50 (■) μM MeSSCoA in 50 mM phosphate buffer (pH 7.4) at room temperature. Aliquots (4 μl) were withdrawn from the incubation mixture at the indicated times and activity of the enzyme was measured as described in Experimental Procedures.

(B) Acylation of ecFabH was determined by reacting ecFabH (●) or the ~50% active ecFabH-MeSSCoA complex (▲) with [^{14}C]acetyl-CoA and measuring the amount of [^{14}C]acetylated enzyme by liquid scintillation counting.

method permitted estimation of the sequential rates of acylation, as k_{a1} = 0.05 s^{-1} and k_{a2} = 0.005 s^{-1}. These data not only indicate that diacylation of ecFabH does occur, consistent with an ecFabH acetyl-CoA crystal structure which shows acylation of Cys112 in both subunits [25], but also that the second acylation step is slower (10-fold) than the first.

Parallels clearly exist between the biphasic acylation of ecFabH with acetyl-CoA (Figure 4B) and biphasic inhibition with MeSSCoA (Figure 4A). The two-step process is slower for the MeSSCoA inhibitor than for the acetyl-CoA substrate (complete acylation occurs faster than complete inhibition). This slow 50%–100% inhibition step permitted determination of the acylation rate of the second subunit of an ecFabH dimer already modified at one active site with MeSSCoA. We treated the enzyme with excess MeSSCoA for 2 min, at which time it retained approximately 50% activity. As shown (Figure 4B), the rate of acylation of this 50% inhibited ecFabH dimer was dramatically decreased (k_a = 6.6 × 10^{-5} s^{-1}). The dramatic decrease in either inhibitor modification or acylation of the second active site by MeSSCoA and acetyl-CoA, respectively, indicates that the biphasic processes do not reflect intrinsic differences between the two subunits of ecFabH, but rather differences caused by modification of the first subunit. The rate of acylation of the 50% inhibited ecFabH (k_a) is decreased approximately 1000-fold and 100-fold relative to the two acylation steps for the native ecFabH. However, in the presence of malonyl-ACP, the enzyme retains 50% activity and the reaction rate is greater than 0.016 s^{-1}, comparable to that of the native ecFabH dimer (k_{a1} = 0.05 s^{-1}). Because the dramatic decrease in acylation rate for ecFabH modified at one active site cysteine by MeSSCoA is observed only in the absence of malonyl-ACP, this observation suggests that malonyl-ACP is reversing the asymmetry of subunit catalytic activity imposed by prior inhibition or acylation of the first active site.

Crystal Structures of the MeSSCoA-ecFabH Complex

The structures of three complexes of MeSSCoA with ecFabH confirmed the presence of an MeS group on the active site cysteine of one (subunit A) of the two monomers in each of the three crystal dimers. Two inhibition complex structures were determined from preformed crystals soaked in MeSSCoA at two different concentrations (0.16 and 1.7 mM) of the inhibitor. Cocrystals were also obtained by preincubation of the enzyme with 1 mM MeSSCoA to form a complex, followed by crystallization under high ionic strength conditions closely similar to those used for the uninhibited enzyme. The crystal lattices of these three complexes are isomorphous, and in all three samples, the concentration of MeSSCoA was at the high end of the range used for kinetic studies. The molar excess of inhibitor over protein was much higher in the soaks than in the cocrystallization. Interpretation of the electron-density maps was supported by careful iterative fitting and adjustment of occupancies of the ligands, so that there was minimal significant positive or negative residual electron density in the final $mF_o - dF_c$ difference Fourier map.

Electron density for the SMe adduct on the side-chain sulfur of the active site Cys112 is clear and unambiguous in the A subunit of the two soaked structures. This observation confirms the identification of Cys112 as the target residue for this inhibitor (Figure 5A). The SMe group in these structures has an occupancy of 1.0 and 0.8 for the high and low MeSSCoA concentration soaks, respectively, and is sensitively reflected in the electron density of the $mF_o - dF_c$ difference Fourier maps from which it was determined. The MeS group is oriented toward the small hydrophobic pocket composed of the side chains (given for subunit A) Phe87(B), Ala111(A), Leu142(A), Phe157(A), Leu189(A), Leu205(A), and Gly306(A), which has been inferred to constitute the acyl-group binding site in ecFabH. The electron density for the MeS group could not be fit by any of the known sulfoxides, consistent

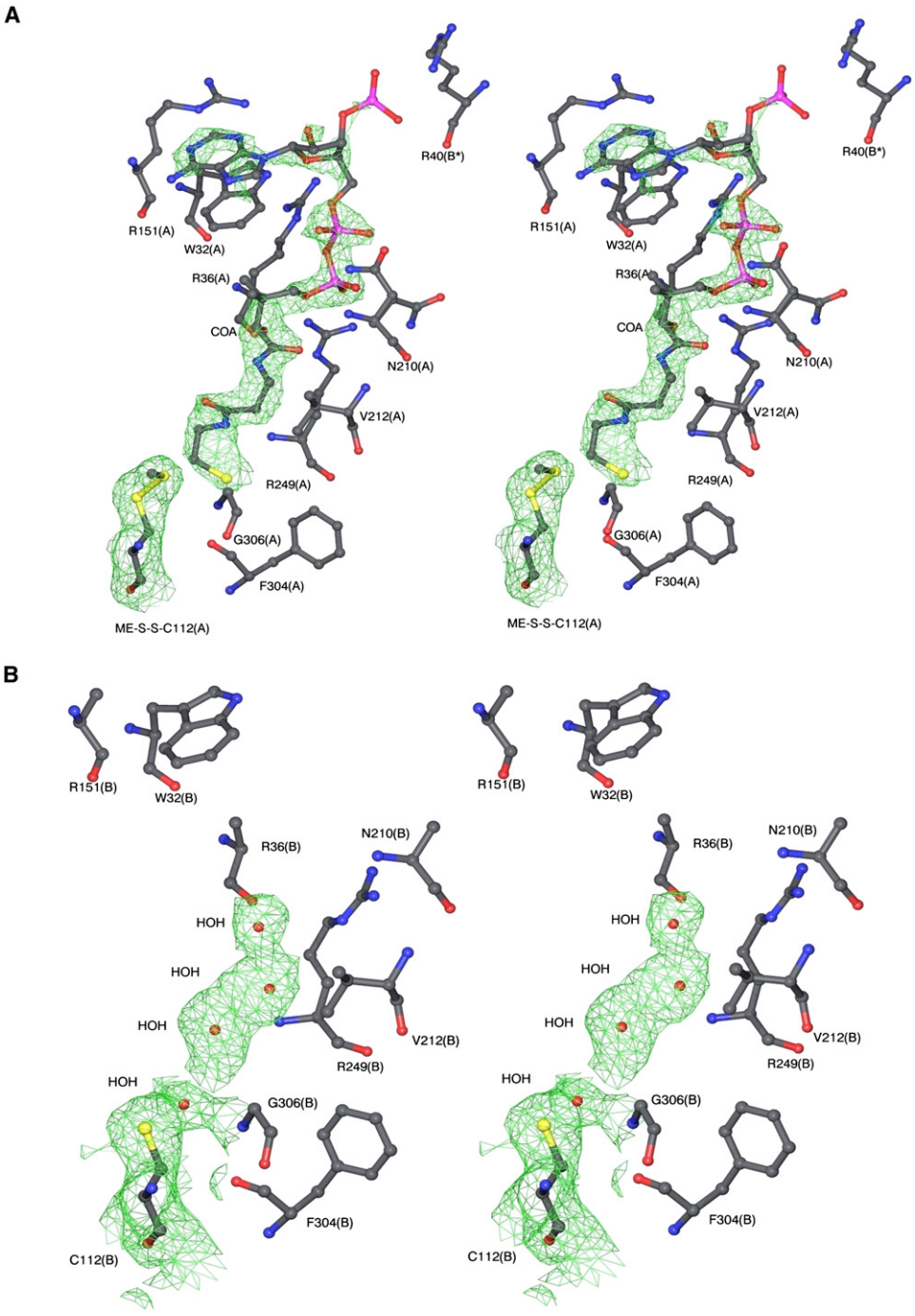

Figure 5. Crystal Structure of the ecFabH-MeSSCoA Soaked Complex

Stereo figure showing electron density for (A) the CoA and MeS-Cys112 in the A subunit of the ecFabH-MeSSCoA (**1**) complex (0.16 mM) contoured at a level of 0.9σ, and (B) electron density of the corresponding site in the B subunit. Electron density of nearby groups is omitted for clarity.

with all previous structures of ecFabH obtained under these and similar conditions, which show Cys112 to be in its reduced form. Like the structures of the soaked complexes, the structure of the cocrystal complex has electron density only in the A site, albeit at lower occupancy (0.3) and consequently less well defined, that can be fit by an SMe adduct on the Cys112 side chain. In contrast to the soaked complexes, there is a conditionally occupied solvent molecule site in the oxyanion hole of the cocrystal that overlaps the MeS density in this structure.

In the B subunit active site of all three ecFabH structures determined, there is a single peak of electron density in the

oxyanion hole (Figure 5B). This peak has been identified as a solvent ligand, either a water or possibly a hydroxide ion [23, 25, 29], that is stabilized in its binding site by stereochemical and charge similarity to the substrate acyl-group oxyanion intermediate. This site is conditionally occupied in the A subunit of the cocrystal structure, but there is no evidence for any solvent in the oxyanion hole of the high-occupancy methylthiolated A subunits in the two soaked complexes.

Almost complete electron density for CoA is present in the A subunit CoA channel (occupancies of 0.7 and 0.6 for high and low MeSSCoA concentration soaks, respectively) for the two inhibitor soaked structures (Figure 5A), with short breaks only at the C5′-O5′ bond of the ribose and at the C5-C6 bond of the adenine ring. The side chains of Trp32 and Arg151 are coplanar and separated to form the stacked sandwich structure around the adenine ring of the CoA that is observed in all other FabH-CoA complexes [23, 25, 28]. The 3′ phosphate of the CoA adenine nucleotide in the A subunit forms an electrostatic interaction with the guanidinium side chain of Arg40(B) from the B subunit of a lattice-related dimer. The pyrophosphoryl group of CoA makes multiple hydrogen-bond and electrostatic interactions: with the Asn210 side-chain amido group, the Arg249 guanidinium side chain, and two solvent molecules. The free terminal thiol group of CoA is oriented toward Phe304, Ala246, and Val212 at the foot of the CoA channel, but it and the pantetheinate group make no polar interactions with the protein. In the cocrystal complex structure, the very limited density in the CoA channel cannot be fit by all or part of a CoA, and was modeled as solvent water. Despite the absence of clearly ordered CoA in the A-site channel of the cocrystal complex structure, the Trp32-Arg151 sandwich at the mouth is open, indicating disordered occupancy of this site by the CoA adenine. The B channel of all three structures shows no connected density that could be fit by all or part of a CoA, and the Trp32 and Arg151, which form the sandwich around the adenine of CoA, are disordered.

Comparison of the structures reported here with that reported for ecFabH in complex (RCSB accession number 1HND) with CoA [21, 25] shows differences in conformation of the pantetheinate-mercaptoethylamine segments of the cofactor. In the MeSSCoA-ecFabH structures, there are no hydrogen bonds or polar interactions between CoA and the enzyme, whereas in the ecFabH-CoA complex, there was a single hydrogen bond between the amide side chain of Asn247 and the pantetheinate peptide oxygen proximal to the nucleotide end of CoA. Differences in the CoA conformations in these two structures increase down the channel toward the mercaptoethylamine terminus of the cofactor near Cys112. The absence of any strong bonding constraints on CoA within the binding channel (as opposed to the mouth of the channel), also noted in the complex of lauroyl-CoA with a C112A mutant of mtFabH [28], is consistent with the variable and sometimes disordered structures reported for ligand bound in this channel in the few determined FabH-cofactor complex structures.

The half-site occupancy observed in the crystal structures of the MeSSCoA inhibition complexes is consistent with the biphasic inhibition of ecFabH by MeSSCoA in solution. While different lattice environments of the two substrate binding sites may contribute to different affinities for inhibitor binding, formation of the MeSSCoA-ecFabH complex cocrystals with the same half-site bias in subunit occupancy implies that a significant population of half-occupied dimer ecFabH-inhibitor complexes exists in solution. A stabilizing lattice interaction is observed for the CoA product of the inhibition complex in the A active site where the Cys112 is methylthiolated, which likely accounts for the retention of CoA product in that site. There is no evidence for any significant MeS group substitution on the Cys112 of the B-subunit active site at the high concentrations of MeSSCoA used in these soaking experiments, despite its completely unobstructed access to solvent in the crystal lattice. It is also noteworthy that soaking of ecFabH crystals over a 10-fold range of MeSSCoA produced an occupancy difference of 30% for the MeS group in the two A sites with no evidence for any binding of inhibitor in the B site, even at the higher inhibitor concentration. This observation further supports an asymmetry between the two sites of the ecFabH dimer both in solution and in the crystal lattice, extending beyond the different lattice environments of the two subunits.

In contrast to the differences in ligand and solvent occupancy between the two subunits of the ecFabH crystal dimers, the conformations of these two crystallographically nonequivalent subunits are virtually identical (rmsd = 0.44 Å for Cα atoms), except for minor variations in the conformations of the loops from residues 196–201, which lie in different lattice environments in the crystal and are not proximal to the MeS or CoA ligands. There are no side-chain conformational differences between the two subunits of the dimer within the CoA binding channel.

A Model for FabH Catalysis

These studies demonstrate that MeSSCoA inhibits ecFabH by transferring the MeS group to the active site Cys112. This thiol-disulfide exchange process is distinct from the acyl transfer process from acetyl-CoA in the normal catalytic process, and differences between this inhibitor and acetyl-CoA substrate are clearly observed by fluorimetry. However, in both cases the active site thiol is modified, the methyl group occupies the same acyl binding pocket of the enzyme, and the rates of these two processes on native ecFabH are comparable.

Solution and kinetic studies have also revealed that for both the substrate and inhibitor, modification of the second subunit proceeds at a much slower rate. There is virtual identity in conformation between the polypeptide chains of the two monomers of the ecFabH crystal structures reported herein, and also with those previously reported [25], indicating that the slower rate of reaction of the second subunit is not a reflection of a preexisting structural difference between the two subunits. We observe that modification of one subunit by the MeSSCoA inhibitor or acetyl-CoA results in differing effects on the

reactivity of the second subunit. The crystal structures also show a highly ordered solvent in the oxyanion hole of the B subunit of the ecFabH-inhibitor complex, which must be displaced in order for the Cys112 of this subunit to react with either ligand. These observations lead us to propose that the slower rates for modification of this second subunit are a result of changes induced by ligand binding to the first subunit.

We suggest that the apo-ecFabH dimer in solution exists as a distribution of an "open" (partially disordered) and a "closed" (fully ordered) form, the open form having higher affinity for substrate and active site ligands. Binding of a ligand to the partially ordered active site(s) of an open dimer would induce formation of the closed form and shift the distribution toward this conformational state. A previous crystal structure of apo-ecFabH (lacking either added or adventitious ligands) in a tetragonal lattice (RCSB accession number 1HNK), with one monomer per asymmetric unit, may represent the open form of apo-ecFabH [25]. In this structure, four loop regions constituting important parts of the dimer interface and also the substrate binding channel are disordered. In the ordered dimer structures of ecFabH, both liganded and unliganded, these loops from each monomer interact and are ordered. In addition, in this tetragonal form of apo-ecFabH, the functional groups of the active site are perturbed relative to their positions in the ligand complexes, and were inferred to be in a catalytically impaired conformation [25]. These differences in structure cannot be attributed to differences in lattice environment, which is the same for all tetragonal forms, both unliganded and liganded, the latter of which are ordered in these regions. The structural differences between the disordered tetragonal apo-ecFabH structure and the ordered FabH structures extends to the solvent at the active site. The disordered tetragonal apo-ecFabH structure has solvent near but not in the oxyanion hole of the active site, its distances from the hydrogen-bond donors of this site being too long for stable hydrogen bonds.

It has been argued [25] that apo-ecFabH is intrinsically disordered and does not achieve its functional conformation until it has bound ligand. Because the flexible loops interact intimately in the stable dimer, we further argue that ordering of those loops through ligand binding to one monomer would cooperatively induce ordering of the counterpart loops in the other monomer, without a requirement for ligand binding to the second monomer. The slow step of interaction of MeSSCoA with ecFabH we observe by fluorimetry could be such a ligand-induced structural organization of the partially disordered apo-ecFabH dimer.

Binding of a ligand at the active site of one of the two partially disordered subunits in an open ecFabH dimer would displace the solvent ligand from the oxyanion hole of that subunit and result in a closed heterodimer with only one active subunit cleared of solvent in its oxyanion hole. Binding of a substrate or inhibitor ligand to the second subunit would be hindered, both by its transition to the lower affinity closed form and by retention of bound solvent in its oxyanion hole. Ligand access to the active site of the second subunit in its closed form may still occur through the CoA channel, but is likely to be much slower than that with the open form. The kinetic evidence indicates that access to the second subunit is reduced more when the ligand binding in the first subunit is the MeSSCoA inhibitor rather than acyl-CoA. Although there are structural and reactivity differences between this substrate and inhibitor, it is not clear which are critical in conferring this difference in reactivity on the second active site.

Our model for ecFabH catalysis thus involves ligand binding to one subunit accompanied by modification of the Cys122 active site and transition to a lower-affinity closed heterodimer with differential catalytic competence in the second subunit. The dramatic increase in acylation rate of a closed ecFabH-MeSSCoA heterodimer with acetyl-CoA which occurs in the presence of malonyl-ACP suggests that this substrate causes a shift to a higher-affinity open heterodimer. In the normal ecFabH-catalyzed process with acetyl-CoA, a shift to the open heterodimer form by malonyl-ACP would facilitate both the subsequent Claisen condensation and eventual product release and restore the enzyme to its starting state.

SIGNIFICANCE

Previous studies of FabH enzymes have focused on acyl-group substrate specificity, enzyme structure, and mutational analysis to probe the role of three catalytic residues [23, 25, 46, 47]. An understanding of the kinetics of each catalytic step and any associated conformational changes, as well as of the role of each FabH subunit in these, remains largely undetermined. As a result, there are a number of observations regarding FabH and related enzymes that have not been incorporated into the knowledge base of this enzyme. These include the relatively poor activity of FabH enzymes as transacylases (using ACP as opposed to malonyl-ACP as the second substrate), the changes in relative acyl-CoA specificities of FabH enzymes conferred by noncognate malonyl-ACP substrates, and acylation rates for condensing enzymes which are slower than the observed overall catalytic process [29, 31]. These studies support and expand a previous proposal that apo-ecFabH exists in a partially disordered form that becomes ordered on binding of substrate. Our results indicate that ecFabH exists in a distribution of "open" and "closed" dimer forms and that reaction of a substrate (acetyl-CoA) or inhibitor (MeSSCoA) molecule with one subunit of the dimer induces concomitant reduced affinity of the second subunit for either ligand. This negative cooperativity is observed only in the absence of malonyl-ACP, indicating that binding of this second substrate leads to a disordering of the ecFabH structure and a shift in its distribution toward the open form. This elaborated mechanism of FabH action may help to rationalize previously inexplicable observations and

provide a basis for the design of new experiments to test it.

EXPERIMENTAL PROCEDURES

Materials

Malonyl-CoA, long-chain acyl-CoAs, imidazole, dithiothreitol (DTT), and Ellman's reagent (Sigma); coenzyme A trihydrate (Fluka); reverse-phase thin-layer chromatography sheets (RP-TLC) with fluorescent indicator at 254 nm (C18, RP-18 $F_{254\,s}$) (Merck); alkyl methanethiosulfonate (TRC Biomedical Research Chemicals); [1-^{14}C]acetyl-CoA (specific activity, 50 mCi/mmol) (Moravek Biochemicals); [2-^{14}C]malonyl-CoA (ARC-528, specific activity 55 mCi/mmol) (American Radiolabel); C18 cartridge (Supelco, Discovery DSC-18LT, bed wt 500 mg, 3 ml volume). The ecFabH expression plasmid was kindly provided by Pfizer.

Chemical Synthesis

S-Sec-Butyl-Methanethiosulfonate

Prepared as reported earlier [48].

Methyl-CoA Disulfide 1

A solution of coenzyme A trihydrate (10 mg, 12.1 μmol) and methyl-methanethiosulfonate (12 mg, 95.2 μmol, 8 equivalents) in anhydrous methanol (0.7 ml) was stirred at room temperature for 3 hr under nitrogen. Reaction progress was monitored by HPLC (or RP-TLC) using UV detection at 254 nm. After completion of the reaction, methanol was removed in vacuo and the resulting solid residue was washed thoroughly with hexane (2 × 0.5 ml) and methylene chloride (2 × 0.5 ml) to extract unreacted methylmethanethiosulfonate and other side products. The solid residue was dissolved in a minimal amount of methanol and applied directly to a Supelco C18 cartridge preequilibrated with water. The column was eluted (by applying positive pressure) with a gradient of methanol in water (0%–100%), and the fractions containing the desired product (as determined by HPLC or RP-TLC) were pooled and concentrated in vacuo to give the desired methyl-CoA disulfide (**1**) (7 mg, 71%) as a white puffy solid: TLC R_f = 0.53 (C18 silica, 33% MeOH/H_2O).

Alkyl-CoA Disulfides 2–5

The alkyl-CoA disulfides **2**–**5** were prepared as described above for methyl-CoA disulfide **1** using the appropriate alkyl methanethiosulfonate.

Enzyme Expression and Purification

ecFabH and *Streptomyces glaucescens* FabD (sgFabD) proteins were overexpressed in *E. coli* with an N-terminal polyhistidine tag and subsequently purified by metal-chelation chromatography as described previously [30, 37]. Purified mtFabH was prepared as described earlier [28].

FabH Enzyme Assays

ecFabH assays were carried out using a standard coupled trichloroacetic acid precipitation assay, which determines the rate of formation of radiolabeled 3-ketoacyl-ACP from malonyl-ACP and radiolabeled acetyl-CoA [10, 33]. In this coupled assay, sgFabD is used to generate the malonyl-ACP substrate (MACP) from malonyl-CoA and ACP [45]. The mtFabH assay was a modification of an assay procedure used by Brown et al. [29] substituting malonyl-CoA for MACP. A typical 20 μl assay consisted of 12.5 μM lauroyl-CoA, 12.5–50 nCi [2-^{14}C]-malonyl-CoA (specific activity 55 mCi/mmol) in 100 mM sodium phosphate buffer (pH 7.0). The reaction was initiated by addition of 0.2 μg of mtFabH. After incubation at 37°C for 60 min, the reaction was quenched and reduced by adding 500 μl of 5 mg/ml $NaBH_4$ in 100 mM K_2HPO_4, 100 mM KCl, 30% tetrahydrofuran and keeping it at 37°C for 20–30 min. The radiolabeled 3-ketoacyl-CoA thioester product was reduced to the corresponding acyl-1,2-diols, extracted with 500 μl of toluene, and quantitated using a liquid scintillation counter. Alkyl-CoA disulfides were either preincubated with the ecFabH enzymes for 15 min or added at the same time as the substrates. The IC_{50} (concentration of inhibitor at which 50% inhibition of FabH is achieved) was determined by duplicate assays with a minimum of six concentrations of inhibitor. The IC_{50} values were calculated with Grafit 4.012 (Erithacus Software).

Stopped-Flow Fluorimetry

A microvolume stopped-flow reaction analyzer, the SF-61 DX2 Double Mixing Stopped Flow system (Hi-Tech Scientific), equipped with a fluorescence detector and a thermostated cell, was used to monitor the changes in Trp fluorescence due to the reaction of ecFabH with MeSS-CoA (**1**). Measurements were carried out in 50 mM phosphate buffer (pH 7.4) at 25°C. The excitation wavelength was set at 290 nm, and the progress of the reaction was monitored by measuring the changes in Trp fluorescence emission through a 320 nm cutoff filter. Interaction of ecFabH with **1** resulted in two distinct changes in Trp fluorescence emission: an initial fast decrease followed by a slow increase. Both fast and slow phases were analyzed separately using SigmaPlot 8.0 (SPSS) for Windows. For the fast step, a decrease in the Trp fluorescence emission was fitted to a single exponential equation, $F_t = A + B\ e^{-(kobs)t}$, where F_t is the fluorescence at time t, A is an offset, B is the amplitude, and k_{obs} is the pseudo-first-order rate constant. The dependence of k_{obs} on [**1**] was fit to the hyperbolic equation $k_{obs} = k_{lim}*[\mathbf{1}]/(K_{0.5} + [\mathbf{1}])$, where k_{lim} is the limiting rate constant of the first step and $K_{0.5}$ is the concentration of MeSSCoA (**1**) at half-saturation. For the slow second step, the observed increase in Trp fluorescence emission was fit to the equation $F_t = A + B\ (1 - e^{-kobst})$, where F_t is fluorescence emission at time t, A is an offset, and B is the amplitude. Values of k_{obs} were plotted against reactant concentration and the linear equation was fit to the data to obtain the k_{slow} value.

Time-Dependent Inhibition

The time course for inactivation of ecFabH by a range of MeSSCoA (**1**) concentrations (1–50 μM) was conducted by incubation in 50 mM sodium phosphate buffer (pH 7.4) at room temperature and withdrawing samples for assay at specific time points. Activity was expressed as a fraction of activity remaining relative to a control experiment carried out in the absence of inhibitor. Time dependencies of activity of FabH incubated with **1** were analyzed using SigmaPlot 8.0 software (SPSS) for Windows. A double exponential equation ($A_t = A_0\ e^{-k'obst} + B_0\ e^{-kobst}$) was fitted to the observed decrease in ecFabH activity with time, where ($A_0 + B_0$) and A_t are activities of FabH at times zero and t, and k'_{obs} and k_{obs} are the observed rate constants for the fast and slow loss of ecFabH activity, respectively. The values of k_{obs} were plotted versus [**1**] and fit by a hyperbolic equation, $k_{obs} = k_{i2}*[\mathbf{1}]/(K_i + [\mathbf{1}])$, where K_i is the dissociation constant of the FabH-**1** complex and k_{i2} is the rate constant of the slow FabH inhibition step. The rate constant for the fast inhibition step, k_{i1}, was estimated from the values of k_{obs} at saturation (10 and 50 μM of MeSSCoA).

Reversibility Tests

A solution of ecFabH (500 μl of a 1.3 μM solution in 50 mM sodium phosphate buffer [pH 7.4]) was preincubated with MeSSCoA (**1**) (6.6 μl of a 10 mM solution in water; ratio of inhibitor to enzyme, 100:1) for 30 min at room temperature. A control solution containing the ecFabH enzyme in buffer and 6.6 μl of water with no inhibitor was treated in the same manner. Two aliquots from each solution (2 μl each) were withdrawn, and the ecFabH activity was determined under standard assay conditions. The remaining enzyme solutions were dialyzed against 50 mM sodium phosphate buffer (pH 7.4) for 12 hr at 4°C and the enzyme activity was determined. The enzyme solutions were then treated with DTT (10 mM final concentration) for 30 min at room temperature, dialyzed against 50 mM sodium phosphate buffer (pH 7.4) for 3 hr at 4°C, and the enzyme activity was determined under standard conditions (see above).

Acylation Assay of ecFabH

The extent of acylation of ecFabH was determined by measuring the transfer of a radiolabeled acetyl group from [^{14}C]acetyl-CoA to ecFabH. The standard 20 μl reaction mixture contained 50 mM sodium phosphate buffer (pH 7.4) and ecFabH (0.2 nmol of monomer, 10 μM), and the acylation was initiated by adding [^{14}C]acetyl-CoA (2 nmol, 100 μM). The mixture was incubated at room temperature and aliquots were removed at intervals over a 10 min period. For each sample, the reaction was stopped by addition of 10% trichloroacetic acid and analyzed in the standard way using liquid scintillation counting. A plot of the amount of radiolabeled protein versus time was constructed and used to estimate k_{a1} and k_{a2}.

Acylation Assay of an ~50% Active ecFabH-MeSSCoA Complex

ecFabH (0.2 nmol of monomer, 10 μM) was incubated with MeSSCoA (10 nmol, 500 μM) in 50 mM sodium phosphate buffer (pH 7.4) at room temperature for 2 min. An aliquot of this partially inhibited ecFabH (5 μM) MeSSCoA mixture was incubated with [^{14}C]acetyl-CoA (50 μM) and malonyl-ACP (4 μM), and shown in a standard FabH assay [10, 33] to reproducibly retain approximately 50% of the activity of the native protein. An acylation assay of this same partially inhibited ecFabH (5 μM) MeSSCoA was simultaneously carried out over a range of [^{14}C]acetyl-CoA concentrations (50–500 μM). These two assays were repeated multiple times with different enzyme-acetyl-CoA ratios with the same result that the overall rate for the catalytic process (>0.016 s^{-1}) was approximately 240-fold higher than the acylation rate ($k_a = 6.6 \times 10^{-5}$ s^{-1}).

X-Ray Structure Determination of the ecFabH-MeSSCoA (1) Complexes

Crystals of ecFabH and the ecFabH-MeSSCoA complex were obtained by the hanging drop method at room temperature. For the former, drops composed of equal volumes of a solution of 15 mg/ml ecFabH in 20 mM Tris (pH 7.4) and a reservoir solution (0.1 M sodium HEPES [pH 7.5], 1.6–1.9 M ammonium sulfate, 2% PEG-400) were equilibrated against the reservoir solution. Optimal crystals of the ecFabH-MeSSCoA complex were obtained by mixing 2.2 μl of protein-inhibitor complex solution with 2.2 μl of reservoir solution (0.1 M sodium HEPES [pH 7.0], 1.7 M ammonium sulfate, 2% PEG-400) and equilibrating the drops against the reservoir. The protein-inhibitor complex was prepared by mixing MeSSCoA (**1**) (10 mM solution in water) with ecFabH enzyme solution (10 mg/ml in 20 mM sodium HEPES [pH 7.2]) at a molar ratio of protein:inhibitor = 1:4 and incubated for several hours at 4°C. Conditions used for crystallization of both ecFabH and the ecFabH-MeSSCoA (**1**) complex are similar to those described for native crystals [23], and the lattice of the complex is closely similar to that of the native crystals (a = 64.38, b = 82.04, c = 121.67, P212121, two monomers per asymmetric unit). Crystals of the ecFabH-MeSSCoA complex diffract to 2.0 Å resolution. Crystals of ecFabH stabilized in 0.1 M sodium HEPES (pH 7.5), 2.2 M ammonium sulfate, 2% PEG-400 were soaked for 20–24 hr in a cold room with the same solution containing either 0.16 mM or 1.7 mM MeSSCoA. These crystals also diffracted to about 2 Å resolution.

X-ray data were collected at 100K using a Molecular Structure Corporation (MSC) X-Stream Cryogenic Crystal Cooler system and an R-Axis IV^{2+} image plate detector on a Rigaku MicroMax-007 X-ray source equipped with MSC Varimax confocal optics operating at 40 kV and 20 mA. The data set was processed with the MSC d*TREK software program. Prior to data collection, crystals were first washed in cryoprotectant solution containing 1.6 M ammonium sulfate (for the complex) or 2.2 M ammonium sulfate (for preformed, soaked crystals), 2% PEG-400, 0.5 mM methyl-CoA disulfide, 100 mM sodium HEPES (pH 7.0), 5% glycerol, followed by transfer to similar solutions with 12% and 17% glycerol.

An initial model of the unliganded ecFabH dimer (RCSB accession number 1HND) was placed in the unit cell of the ecFabH-MeSSCoA crystal with rigid body refinement as implemented in CNS version 1.0. This model was refined iteratively by cycles of simulated annealing with torsion angle dynamics as implemented in CNS version 1.0 coupled with TLS [49] and positional refinement in REFMAC5 [50], followed by manual rebuilding into 2 $mF_o - dF_c$, $mF_o - dF_c$, and 2 $mF_o - dF_c$ composite omit maps using the graphics programs TOM [51, 52] and Xfit [53]. In the final stages of the refinement, 200 water molecules were added to the structure based on the presence of peaks with intensities of >3σ in an $mF_o - dF_c$ difference Fourier map. During refinement, residue geometries were monitored via PROCHECK [54] and WHATCHECK [55], whereas nonbonded contacts were monitored via PROBE [56] as integrated with Xfit. Model coordinate errors were estimated via Cruikshank's diffraction precision indicator as implemented in SFCHECK [57].

Supplemental Data

Supplemental Data include four figures and one table and are available at http://www.chembiol.com/cgi/content/full/14/5/513/DC1/.

ACKNOWLEDGMENTS

This work was supported by a grant from the NIH (AI52230).

Received: August 23, 2006
Revised: February 26, 2007
Accepted: March 16, 2007
Published: May 29, 2007

REFERENCES

1. Wakil, S.J. (1989). Fatty acid synthase, a proficient multifunctional enzyme. Biochemistry *28*, 4523–4530.
2. Joshi, A.K., Witkowski, A., and Smith, S. (1997). Mapping of functional interactions between domains of the animal fatty acid synthase by mutant complementation in vitro. Biochemistry *36*, 2316–2322.
3. Schweizer, E., and Hofmann, J. (2004). Microbial type I fatty acid synthases (FAS): major players in a network of cellular FAS systems. Microbiol. Mol. Biol. Rev. *68*, 501–517.
4. Clough, R.C., Matthis, M., Barnum, S.R., and Jaworski, J.G. (1992). Purification and characterization of 3-ketoacyl-acyl carrier protein synthase III from spinach. A condensing enzyme utilizing acetyl coenzyme A to initiate fatty acid synthesis. J. Biol. Chem. *267*, 20992–20998.
5. Rock, C.O., and Cronan, J.E. (1996). *Escherichia coli* as a model for the regulation of dissociable (type-II) fatty acid biosynthesis. Biochim. Biophys. Acta *1302*, 1–16.
6. Surolia, N., and Surolia, A. (2001). Triclosan offers protection against blood stages of malaria by inhibiting enoyl-ACP reductase of *Plasmodium falciparum*. Nat. Med. *7*, 167–173.
7. Wang, J., Soisson, S.M., Young, K., Shoop, W., Kodali, S., Galgoci, A., Painter, R., Parthasarathy, G., Tang, Y.S., Cummings, R., et al. (2006). Platensimycin is a selective FabF inhibitor with potent antibiotic properties. Nature *441*, 358–361.
8. Heath, R.J., White, S.W., and Rock, C.O. (2001). Lipid biosynthesis as a target for antibacterial agents. Prog. Lipid Res. *40*, 467–497.
9. Prigge, S.T., He, X., Gerena, L., Waters, N.C., and Reynolds, K.A. (2003). The initiating steps of a type II fatty acid synthase in *Plasmodium falciparum* are catalyzed by pfACP, pfMCAT, and pfKASIII. Biochemistry *42*, 1160–1169.
10. Tsay, J.T., Oh, W., Larson, T.J., Jackowski, S., and Rock, C.O. (1992). Isolation and characterization of the β-keto-acyl carrier protein synthase III gene (*fabH*) from *Escherichia coli* K-12. J. Biol. Chem. *267*, 6807–6814.
11. Edwards, P., Nelsen, J.S., Metz, J.G., and Dehesh, K. (1997). Cloning of the fabF gene in an expression vector and in vitro characterization of recombinant fabF and fabB encoded enzymes from *Escherichia coli*. FEBS Lett. *402*, 62–66.

12. Zhang, Y.M., White, S.W., and Rock, C.O. (2006). Inhibiting bacterial fatty acid synthesis. J. Biol. Chem. *281*, 17541–17544.
13. Price, A.C., Choi, K.H., Heath, R.J., Li, Z., White, S.W., and Rock, C.O. (2001). Inhibition of β-ketoacyl-acyl carrier protein synthases by thiolactomycin and cerulenin. Structure and mechanism. J. Biol. Chem. *276*, 6551–6559.
14. Kauppinen, S., Siggaard-Andersen, M., and von Wettstein-Knowles, P. (1988). β-ketoacyl-ACP synthase I of *Escherichia coli*: nucleotide sequence of the fabB gene and identification of the cerulenin binding residue. Carlsberg Res. Commun. *53*, 357–370.
15. Dolak, L.A., Castle, T.M., Truesdell, S.E., and Sebek, O.K. (1986). Isolation and structure of antibiotic U-68,204, a new thiolactone. J. Antibiot. (Tokyo) *39*, 26–31.
16. Nishida, I., Kawaguchi, A., and Yamada, M. (1986). Effect of thiolactomycin on the individual enzymes of the fatty acid synthase system in *Escherichia coli*. J. Biochem. (Tokyo) *99*, 1447–1454.
17. Daines, R.A., Pendrak, I., Sham, K., Van Aller, G.S., Konstantinidis, A.K., Lonsdale, J.T., Janson, C.A., Qiu, X., Brandt, M., Khandekar, S.S., et al. (2003). First X-ray cocrystal structure of a bacterial FabH condensing enzyme and a small molecule inhibitor achieved using rational design and homology modeling. J. Med. Chem. *46*, 5–8.
18. He, X., Reeve, A.M., Desai, U.R., Kellogg, G.E., and Reynolds, K.A. (2004). 1,2-dithiole-3-ones as potent inhibitors of the bacterial 3-ketoacyl acyl carrier protein synthase III (FabH). Antimicrob. Agents Chemother. *48*, 3093–3102.
19. Alhamadsheh, M.M., Waters, N.C., Huddler, D.P., Kreishman-Deitrick, M., Florova, G., and Reynolds, K.A. (2007). Synthesis and biological evaluation of thiazolidine-2-one 1,1-dioxide as inhibitors of *Escherichia coli* β-ketoacyl-ACP-synthase III (FabH). Bioorg. Med. Chem. Lett. *17*, 879–883.
20. Nie, Z., Perretta, C., Lu, J., Su, Y., Margosiak, S., Gajiwala, K.S., Cortez, J., Nikulin, V., Yager, K.M., Appelt, K., and Chu, S. (2005). Structure-based design, synthesis, and study of potent inhibitors of β-ketoacyl-acyl carrier protein synthase III as potential antimicrobial agents. J. Med. Chem. *48*, 1596–1609.
21. Qiu, X., Janson, C.A., Konstantinidis, A.K., Nwagwu, S., Silverman, C., Smith, W.W., Khandekar, S., Lonsdale, J., and Abdel-Meguid, S.S. (1999). Crystal structure of β-ketoacyl-acyl carrier protein synthase III. A key condensing enzyme in bacterial fatty acid biosynthesis. J. Biol. Chem. *274*, 36465–36471.
22. Khandekar, S.S., Konstantinidis, A.K., Silverman, C., Janson, C.A., McNulty, D.E., Nwagwu, S., Van Aller, G.S., Doyle, M.L., Kane, J.F., Qiu, X., and Lonsdale, J. (2000). Expression, purification, and crystallization of the *Escherichia coli* selenomethionyl β-ketoacyl-acyl carrier protein synthase III. Biochem. Biophys. Res. Commun. *270*, 100–107.
23. Davies, C., Heath, R.J., White, S.W., and Rock, C.O. (2000). The 1.8 Å crystal structure and active-site architecture of β-ketoacyl-acyl carrier protein synthase III (FabH) from *Escherichia coli*. Struct. Fold. Des. *8*, 185–195.
24. Scarsdale, J.N., Kazanina, G., He, X., Reynolds, K.A., and Wright, H.T. (2001). Crystal structure of the *Mycobacterium tuberculosis* β-ketoacyl-acyl carrier protein synthase III. J. Biol. Chem. *276*, 20516–20522.
25. Qiu, X., Janson, C.A., Smith, W.W., Head, M., Lonsdale, J., and Konstantinidis, A.K. (2001). Refined structures of β-ketoacyl-acyl carrier protein synthase III. J. Mol. Biol. *307*, 341–356.
26. Zhang, Y.M., Rao, M.S., Heath, R.J., Price, A.C., Olson, A.J., Rock, C.O., and White, S.W. (2001). Identification and analysis of the acyl carrier protein (ACP) docking site on β-ketoacyl-ACP synthase III. J. Biol. Chem. *276*, 8231–8238.
27. Qiu, X., Choudhry, A.E., Janson, C.A., Grooms, M., Daines, R.A., Lonsdale, J.T., and Khandekar, S.S. (2005). Crystal structure and substrate specificity of the β-ketoacyl-acyl carrier protein synthase III (FabH) from *Staphylococcus aureus*. Protein Sci. *14*, 2087–2094.
28. Musayev, F., Sachdeva, S., Scarsdale, J.N., Reynolds, K.A., and Wright, H.T. (2005). Crystal structure of a substrate complex of *Mycobacterium tuberculosis* β-ketoacyl-acyl carrier protein synthase III (FabH) with lauroyl-coenzyme A. J. Mol. Biol. *346*, 1313–1321.
29. Brown, A.K., Sridharan, S., Kremer, L., Lindenberg, S., Dover, L.G., Sacchettini, J.C., and Besra, G.S. (2005). Probing the mechanism of the *Mycobacterium tuberculosis* β-ketoacyl-acyl carrier protein synthase III mtFabH: factors influencing catalysis and substrate specificity. J. Biol. Chem. *280*, 32539–32547.
30. He, X., Mueller, J.P., and Reynolds, K.A. (2000). Development of a scintillation proximity assay for β-ketoacyl-acyl carrier protein synthase III. Anal. Biochem. *282*, 107–114.
31. McGuire, K.A., Siggaard-Andersen, M., Bangera, M.G., Olsen, J.G., and von Wettstein-Knowles, P. (2001). β-ketoacyl-[acyl carrier protein] synthase I of *Escherichia coli*: aspects of the condensation mechanism revealed by analyses of mutations in the active site pocket. Biochemistry *40*, 9836–9845.
32. Smirnova, N., and Reynolds, K.A. (2001). Engineered fatty acid biosynthesis in *Streptomyces* by altered catalytic function of β-ketoacyl-acyl carrier protein synthase III. J. Bacteriol. *183*, 2335–2342.
33. Han, L., Lobo, S., and Reynolds, K.A. (1998). Characterization of β-ketoacyl-acyl carrier protein synthase III from *Streptomyces glaucescens* and its role in initiation of fatty acid biosynthesis. J. Bacteriol. *180*, 4481–4486.
34. Choi, K.H., Kremer, L., Besra, G.S., and Rock, C.O. (2000). Identification and substrate specificity of β-ketoacyl (acyl carrier protein) synthase III (mtFabH) from *Mycobacterium tuberculosis*. J. Biol. Chem. *275*, 28201–28207.
35. Choi, K.H., Heath, R.J., and Rock, C.O. (2000). β-ketoacyl-acyl carrier protein synthase III (FabH) is a determining factor in branched-chain fatty acid biosynthesis. J. Bacteriol. *182*, 365–370.
36. Khandekar, S.S., Gentry, D.R., Van Aller, G.S., Warren, P., Xiang, H., Silverman, C., Doyle, M.L., Chambers, P.A., Konstantinidis, A.K., Brandt, M., et al. (2001). Identification, substrate specificity, and inhibition of the *Streptococcus pneumoniae* β-ketoacyl-acyl carrier protein synthase III (FabH). J. Biol. Chem. *276*, 30024–30030.
37. He, X., and Reynolds, K.A. (2002). Purification, characterization, and identification of novel inhibitors of the β-ketoacyl-acyl carrier protein synthase III (FabH) from *Staphylococcus aureus*. Antimicrob. Agents Chemother. *46*, 1310–1318.
38. Currier, S.F., and Mautner, H.G. (1976). Evidence for a thiol reagent inhibiting choline acetyltransferase by reacting with the thiol group of coenzyme A forming a potent inhibitor. Biochem. Biophys. Res. Commun. *69*, 431–436.
39. Currier, S.F., and Mautner, H.G. (1977). Interaction of analogues of coenzyme A with choline acetyltransferase. Biochemistry *16*, 1944–1948.
40. Rossier, J. (1977). Acetyl-coenzyme A and coenzyme A analogues. Their effects on rat brain choline acetyltransferase. Biochem. J. *165*, 321–326.
41. Mautner, H.G., and Currier, S.F. (1978). Studies on the mechanism of action of choline acetyltransferase. Adv. Behav. Biol. *24*, 197–206.
42. Weber, B.H., Hariri, M., Martin, D., and Driskell, W.J. (1979). Enzymic properties of choline acetyltransferase from heads of *Drosophila melanogaster*. J. Neurochem. *32*, 1597–1598.

43. Mautner, H.G., Merrill, R.E., Currier, S.F., and Harvey, G. (1981). Interaction of aromatic dyes with the coenzyme A binding site of choline acetyltransferase. J. Med. Chem. *24*, 1534–1537.
44. Della Ragione, F., Erwin, B.G., and Pegg, A.E. (1983). Studies of the acetyl-CoA-binding site of rat liver spermidine/spermine N1-acetyltransferase. Biochem. J. *213*, 707–712.
45. Florova, G., Kazanina, G., and Reynolds, K.A. (2002). Enzymes involved in fatty acid and polyketide biosynthesis in *Streptomyces glaucescens*: role of FabH and FabD and their acyl carrier protein specificity. Biochemistry *41*, 10462–10471.
46. Jackowski, S., Murphy, C.M., Cronan, J.E., and Rock, C.O. (1989). Acetoacetyl-acyl carrier protein synthase. A target for the antibiotic thiolactomycin. J. Biol. Chem. *264*, 7624–7629.
47. Heath, R.J., and Rock, C.O. (1996). Inhibition of β-ketoacyl-acyl carrier protein synthase-III (FabH) by acyl-acyl carrier protein in *Escherichia coli*. J. Biol. Chem. *271*, 10996–11000.
48. Salvadori, P., Lardicci, L., and Stagi, M. (1968). Optically active aliphatic thiols and thioethers. Gazz. Chim. Ital. *98*, 1400–1416.
49. Brunger, A.T., Adams, P.D., Clore, G.M., DeLano, W.L., Gros, P., Grosse-Kunstleve, R.W., Jiang, J.S., Kuszewski, J., Nilges, M., Pannu, N.S., et al. (1998). Crystallography & NMR System: a new software suite for macromolecular structure determination. Acta Crystallogr. D Biol. Crystallogr. *54*, 905–921.
50. Murshudov, G.N., Vagin, A.A., Lebedev, A., Wilson, K.S., and Dodson, E.J. (1999). Efficient anisotropic refinement of macromolecular structures using FFT. Acta Crystallogr. D Biol. Crystallogr. *55*, 247–255.
51. Cambillau, C., and Horjales, E. (1987). TOM: a FRODO subpackage for protein-ligand fitting with interactive energy minimization. J. Mol. Graph. *5*, 174–177.
52. Kleywegt, G.J., and Jones, A.T. (1997). Model building and refinement practice. Methods Enzymol. *277*, 208–230.
53. McRee, D.E. (1999). XtalView/Xfit—a versatile program for manipulating atomic coordinates and electron density. J. Struct. Biol. *125*, 156–165.
54. Laskowski, R.A., MacArthur, M.W., Moss, D.S., and Thornton, J.M. (1993). PROCHECK: a program to check the stereochemical quality of protein structures. J. Appl. Cryst. *26*, 283–291.
55. Hooft, R.W., Vriend, G., Sander, C., and Abola, E.E. (1996). Errors in protein structures. Nature *381*, 272.
56. Word, J.M., Lovell, S.C., LaBean, T.H., Taylor, H.C., Zalis, M.E., Presley, B.K., Richardson, J.S., and Richardson, D.C. (1999). Visualizing and quantifying molecular goodness-of-fit: small-probe contact dots with explicit hydrogen atoms. J. Mol. Biol. *285*, 1711–1733.
57. Vaguine, A.A., Richelle, J., and Wodak, S.J. (1999). SFCHECK: a unified set of procedures for evaluating the quality of macromolecular structure-factor data and their agreement with the atomic model. Acta Crystallogr. D Biol. Crystallogr. *55*, 191–205.

Accession Numbers

Coordinates and structure factors for the ecFabH-MeSSCoA complex crystal structure have been deposited in the RCSB databank under accession number 2GYO.

